Published in final edited form as:
Mol Microbiol. 2010 May ; 76(3): 662–676. doi:10.1111/j.1365-2958.2010.07121.x.

Pleiotropic Function of Intersectin Homolog Cin1 in *Cryptococcus neoformans*

Gui Shen[1], **Amy Whittington**[2], **Kejing Song**[1], and **Ping Wang**[1,2,3,*]

[1] Research Institute for Children, Louisiana State University Health Sciences Center, New Orleans, Louisiana 70118 USA

[2] Department of Microbiology, Immunology, and Parasitology, Louisiana State University Health Sciences Center, New Orleans, Louisiana 70118 USA

[3] Department of Pediatrics, Louisiana State University Health Sciences Center, New Orleans, Louisiana 70118 USA

Summary

The manifestation of virulence traits in *Cryptococcus neoformans* is thought to rely on intracellular transport, a process not fully explored in this pathogenic fungus. Through interaction cloning, we identified a multi-modular protein, Cin1 (cryptococcal intersectin 1), whose domain structure is similar to that of the human endocytic protein ITSN. Cin1 contains an N-terminal EH domain, a central coiled-coil region, a WH2 domain, two SH3 domains, and a C-terminal RhoGEF (DH)-PH domain. Interestingly, alternative mRNA splicing resulted in two Cin1 isoforms, and Cin1 homologs are also restricted to basidiomycetous fungi. Disruption of the *CIN1* gene had a pleiotropic effect on growth, normal cytokinesis, intracellular transport, and the production of several virulence factors. Additionally, Cin1 interacts with cryptococcal Cdc42 and Wsp1 (a WASP homolog) proteins in vitro, suggesting a conserved role in the regulation of the actin cytoskeleton. However, deletion of RhoGEF or SH3 and RhoGEF domains did not result in any phenotypic changes, suggesting that functional redundancy exists in proteins containing similar domains or that the activities by other domains are necessary for Cin1 function. Our study presents the first evidence of a multi-modular protein whose function in intracellular transport underlies the growth, differentiation, and virulence of a pathogenic microorganism.

Introduction

Cryptococcus neoformans is an encapsulated yeast-like pathogenic fungus that infects primarily immunocompromised individuals causing life-threatening meningoencephalitis (Mitchell & Perfect, 1995). This haploid organism has adapted a bipolar mating system consisting of two mating types: MATα and MAT**a,** and genetic cross between the two under laboratory conditions results in recombinant basidiospores. Nevertheless, asexual reproduction through yeast *Saccharomyces cerevisiae*-like budding remains the predominant means of propagation and yeast cells remain the main form of infectious propagles for the fungus. Although detailed studies on the budding process are lacking, Kopecka and colleagues observed that *C. neoformans* not only has a fully developed actin cytoskeleton network, but also maintains yeast-like actin dynamics during mitotic division and asexual reproduction (Kopecka *et al.*, 2001).

*Corresponding author: Ping Wang. pwang@lsuhsc.edu, Phone: (504) 896-2739, Fax: (504) 894-5379.

C. neoformans characteristically produces virulence factors such as an antiphagocytic polysaccharide capsule, the oxidative stress-resistant melanin pigment, and extracellular enzymes such as ureases, and phospholipases (Kozel, 1995, Buchanan & Murphy, 1998, Lengeler *et al.*, 2000). An intracellular transporting event is thought to be important for the production of capsules. Rodrigues and colleagues described the presence of membrane vesicles containing the capsular components: glucuronoxylomannan (GXM) and galactoxylomannan (GalXM) (De Jesus *et al.*, 2009), and Yoneda and colleague also reported that mutation of Sav1, a homolog of *S. cerevisiae* Sec4/Rab8 GTPase involved in post-Golgi secretion, resulted in reduced protein secretion and accumulation of vesicles containing GXM (Yoneda & Doering, 2006). The extracellular enzymes were also thought to be secreted through the trans-cellular transport event (Chen *et al.*, 1996, Cox *et al.*, 2000, Rodrigues *et al.*, 2008, Nosanchuk *et al.*, 2008). Despite their apparent importance, the protein components of the endocytic cycle of endocytosis and exocytosis and their roles in the transport and secretion of capsular materials or enzymatic virulence factors have not been described in this fungus.

Human intersectin is a cytoplasmic membrane-associated protein existing in two isoforms: an ubiquitously distributed short splicing variant, ITSN1s, and a long splicing variant, ITSN1, which is neuronal-specific and expressed only in the brain. ITSN1 is multi-modular protein containing two N-terminal EH domains, a central coiled-coil region, five SH3 domains, a tandem RhoGEF-PH motif, and a C-terminal C2 domain that binds calcium (Figure 1A) (Guipponi *et al.*, 1998, Yamabhai *et al.*, 1998). The EH domain is a protein-protein interaction module of approximately 95 residues found in proteins implicated in endocytosis, vesicle transport, and signal transduction (Confalonieri & Di Fiore, 2002), whereas the WH2 domain, consisting of approximately 18–35 amino acids, has a actin monomer-binding motif and is often found in regulators of the actin cytoskeleton (Symons *et al.*, 1996, Rohatgi *et al.*, 1999, Paunola *et al.*, 2002, Snapper *et al.*, 2001). Additionally, the SH3 domain (~50 amino acids) is found in intracellular or membrane-associated proteins such as phospholipases, tyrosine kinases, and additional proteins such as PI3 Kinase, Ras GTPase activating protein (GAP), Cdc24, and Cdc25 (Mayer, 2001). The RhoGEF domain, also called the DH domain is the structural component of guanine nucleotide exchange factor (GEF) that activates Rho/Rac/Cdc42-like small GTPases to control the actin dynamics, membrane trafficking, and signaling (Cerione & Zheng, 1996, Hussain *et al.*, 2001, Malacombe *et al.*, 2006, Rohatgi et al., 1999, Zamanian & Kelly, 2003, Wang *et al.*, 2005). Lastly, the PH domain, often linked to the RhoGEF domain, is a domain of about 100 residues that occurs in a wide range of proteins involved in intracellular signaling or as constituents of the cytoskeleton (Haslam, 1993; Shaw, 1996; Lemmon, 2000}.

This multi-domain configuration allows ITSN1 to form a macromolecular complex through linkage with proteins of various functions. For example, it binds directly to the human endocytic proteins Epsin 1/Epsin 2, Stoned B/Stonin 2, and proline-rich proteins, such as dynamin, clathrin, synapsin 1 and synaptojanin, to function in endocytosis (Sengar *et al.*, 1999, Martina *et al.*, 2001, Kelly & Phillips, 2005, Roos & Kelly, 1998, Yamabhai et al., 1998, Okamoto *et al.*, 1999). It also stimulates RasGTP levels by recruiting mammalian son-of-sevenless (mSOS), a GEF for Ras, and by forming a complex with Ras in vesicles (Tong *et al.*, 2000, Mohney *et al.*, 2003). More recently, there was evidence indicating that Dap160, a *Drosophila* homolog of ITSN1, bound to aPKC to regulate cell polarity and cell cycle progression (Chabu C, 2008). Importantly, because of its role in neuronal synaptic vesicle endocytosis, ITSN1 overexpression is often associated with Alzheimer's disease and Down syndrome in humans (Pucharcós *et al.*, 1999).

The role of human ITSN1 in exocytosis is exemplified by its presence at the exocytotic sites and its function as a GEF for Cdc42, which facilitates exocytosis in neuroendocrine cells by

stimulating actin assembly, and by binding Snap25, a protein of the exocytotic machinery (Okamoto et al., 1999, Gasman *et al.*, 2004, Malacombe et al., 2006).

In the lower eukaryotic fungi, the *S. cerevisiae* endocytic protein Pan1 contains domains similar to the N-terminus of ITSN1, which includes two EH domains, a coiled-coil region, and a proline-rich region. Pan1 binds to F-actin and promotes actin related proteins Arp2/Arp3 to mediate actin nucleation (Duncan *et al.*, 2001). Moreover, Pan1 was found to regulate endocytosis and to organize cortical actin through interactions with the endocytic protein End3, the clathrin adaptor protein homolog Yap180, the ubiquitin-protein ligase Rsp5 and the early endocytic patch protein Sla2 (Wendland & Emr, 1998, Huang & Cai, 2007, Miliaras *et al.*, 2004).

We discovered Cin1 in a screen for binding partners of Gβ-like/RACK1 protein Gib2 (Palmer *et al.*, 2006) and found that Cin1 exhibits a domain composition similar to that of ITSN1, and more distantly, Pan1. Given the important functions of ITSN1 and Pan1, we characterized the roles of Cin1 in growth, intracellular transport, and formation of several virulence factors.

Results

Identification and characterization of Cin1

In the process of characterizing the Gβ mimic Gib2, we identified a short polypeptide that contains two SH3 domains from a yeast two-hybrid screen (Palmer et al., 2006). Using this sequence as a trace to blast against NCBI database (http://blast.ncbi.nlm.nih.gov/Blast.cgi), we identified it as the internal sequence of an open reading frame (ORF) that encodes a polypeptide of 1978 amino acids of *C. neoformans var. neoformans* (GenBank accession: XP_572068). Sequence analysis indicated that this protein contains multiple domains, including an N-terminal EH domain (E-value: 2.11e-41), a central coiled-coil region, a WH2 domain (E-value: 1.20e-03), and a C-terminal RhoGEF domain (E-value: 1.12e-43), configured similarly to that of human intersectin ITSN1 (Figure 1A). The distinction is that XP_572068 had an internal WH2 domain but lacked a C2 domain, as well as a PH domain. To examine this discrepancy and determine the C-terminal sequence of the ORF, we performed a 3′ RACE (Rapid Amplification of cDNA Ends). A RACE product was obtained using 5′ primer PW700 and 3′ primer AUAP. Sequencing results indicated that the ORF actually encodes a protein of 2004 amino acids (GenBank accession: GU553014). The new ORF revealed the presence of a PH domain (Evalue: 4.04e-09) and confirmed lack of a C2 domain (Figure 1A). Despite a overall low homology in amino acid sequence between GU553014 and ITSN1 (13% identity and 14% homology), there exists a higher degree of sequence homology within the EH (39% identity and 18% similarity), RhoGEF (36% identity and 20% similarity), and PH (25% identity and 15% similarity) domains. Moreover, the N-terminal EH and coiled-coil domain configuration of GU553014 is similar to *S. cerevisiae* endocytic protein Pan1 and there exist 31% identity and 18% similarity in sequence homology within the EH domain. The overall amino acid sequence homology between GU553014 and Pan1 is 12% in identity and 13% in similarity (Figure 1A). We thus named GU553014 as Cin1 for cryptococcal intersectin 1 based on its sharing of more domain conservation and architecture with ITSN1 than Pan1.

Northern blot analysis suggested that there were two major *CIN1* transcripts (data not shown). Indeed, a 3′ RACE with PW1127 and AUAP primers yielded another cDNA fragment whose sequence suggested the existence of a shorter isoform. Sequencing data indicated that alternative splicing of intron #6 at the acceptor site resulted in an ORF encoding a polypeptide of 1282 amino acids (GenBank accession: GU5586282). This short splicing variant (Cin1s) does not contain the DH-PH motif, similar to ITSN1s (Figure 1). In

a semi-quantitative analysis by RT-PCR, *CIN1* transcripts were twice as abundant as that of *CIN1s*, based on the plot density after 25 cycles of amplification (Supplementary Figure 1).

Cin1 sequences are found in divergent but related serotypes A and B strains, and appear to be specific to basidiomycetous fungi. Proteins homologous to Cin1 were found in *Ustilago maydis* (GenBank accession: XP_762160), *Coprinopsis cinerea* (GenBank accession: XP_001839934), and *Phanerochaete chrysosporium* (GenBank accession: XP_001878432), but not in *S. cerevisiae* or other ascomycetes such as *Aspergillus nidulans* or zygomycetes such as *Rhizopus oryzae*.

Cin1 is required for normal cytokinesis and actin distribution

To characterize the function of Cin1, we first generated *cin1* mutants in var. *neoformans* as well as var. *grubii*. The *cin1* null mutant was obtained by disrupting the entire *CIN1* coding region through biolistic genetic transformation. Additionally, two domain-specific mutants, in whom the RhoGEF domain was deleted individually or together with the SH3 domain, were also obtained for var. *neoformans* (Figure 1B, supplementary Figure 2). Severe defects in morphology were seen in the *cin1* mutant. First, cells failed to divide properly, and as a consequence, cell clustering occurred (Figure 2, var. *neoformans* data is shown here and thereafter). Vigorous vortex mixing in the presence of detergents such as Tween 20 (0.5%) or Nonidet P40 (0.1%) did not break cells apart. Second, when stained with nucleic acid dye DAPI, no clearly defined staining pattern was observed. Cells were either not stained or structures resembling mono-, bi-, or multi-nuclei were observed in *cin1* cells (Figure 2A, bottom row), in contrast to the single nucleus found in the wild type cell (Figure 2A, top row). These observations suggested that the *cin1* mutant had defects in cell separation, and possibly, nuclear migration.

To examine actin distribution, cells were stained with rhodamine-conjugated phalloidin, which binds actin filaments. The wild type cell showed random bright fluorescent spots that are cortical actin patches near the plasma membrane, indicating normal distribution of actin (Figure 2B, top row). In contrast, staining of the *cin1* mutant did not reveal similarly distributed actin patches, and instead, no significant staining was observed (Figure 2B, bottom row). In addition, occasional heavily concentrated actin filaments were seen in certain *cin1* cells (data not shown). To substantiate this finding, we randomly countered 100 cells from each of the wild type and mutant strains and recorded the percentage of cells exhibiting normal or abnormal distribution for the actin cable and patches. The actin filaments were visible throughout the cell and the actin patches present near the plasma membrane and in the cytosol in all of wild type cells (100%), whereas only seven mutant cells exhibited actin patches near the plasma membrane (7%) and none were found in the cytosol. Moreover, no actin cable was seen in any of the *cin1* mutant cells observed. These findings collectively suggested that Cin1 plays a role in the distribution of actin and the maintenance of the actin cytoskeleton.

Finally, to determine whether the defect in the actin cytoskeleton resulted in abnormal chitin deposition, we stained the cells with Calcofluor white (CFW), a fluorochrome dye that binds to chitin and is not normally internalized in cells with an intact plasma membrane (Ram & Klis, 2006). The wild type cells exhibited even distribution of CFW around the cell periphery and in the bud neck (Figure 2C, top row), whereas a similar distribution pattern was not observed in the *cin1* mutant. Instead, the distribution of CFW in the *cin1* mutant was not uniformed and was disorganized with patches of the stain near the area where the cells are joined together, indicating abnormal chitin deposition (Figure 2C, bottom row). These observations are consistent with the proposition that Cin1 has a role in the distribution of actin and the normal actin cytoskeleton organization in *C. neoformans*.

The cin1 mutant is defective in growth and endocytosis

In the process of characterizing the *cin1* mutant, we observed that its colonies were smaller than the wild type and other strains on various growth media. In an assay performed by spotting serially diluted cell suspensions onto nutrient-rich YPD and -poor YNB media, the *cin1* mutant indeed exhibited poor growth at 25° C and 30° C, and no growth at 37° C (Figure 3, YNB data not shown). Complementation of the *cin1* mutant strain with the full-length *CIN1* allele (Figure 1C) nearly restored a normal-appearing growth pattern (Figure 3).

In addition, to test whether Cin1 has a role in intracellular transport, we incubated cells with FM4-64, a styryl dye that binds to the vacuolar membrane once internalized by the living cell (Vida & Emr, 1995). The typical staining pattern involves initial rapid absorption of FM4-64 by the plasma membrane, then punctate cytoplasmic staining, and eventual vacuolar membrane staining. For wild type cells, initial staining of the plasma membrane by FM4-64 was not apparent, and, instead, internal staining was seen suggesting rapid intake of the dye (Figure 4, first row). In these cells, FM4-64 was internalized within 15 minutes of incubation, resulting in various bright ring-like stain structures, which are endosomes (Figure 4, fourth row). In contrast, no definitive staining pattern was found in the *cin1* mutant, either at the plasma membrane or in the cytosol up to 30 minutes after exposure to the dye (Figure 4, second and fifth rows). Reintroduction of the *CIN1* gene to the *cin1* mutant restored a staining pattern to near that of the wild type, with apparent initial staining of the plasma membrane and subsequent staining of endosomes (Figure 4, third and sixth rows).

The cin1 mutant is sterile

In *C. neoformans*, mating is a multiple-step process consisting of pheromone induced conjugation tube formation, formation of mating-specific dikaryotic filaments, meiosis and mitosis (Wang & Heitman, 1999, Lengeler et al., 2000). Since the *cin1* mutant is defective in growth, cytokinesis, and intracellular transport, we were intrigued to assess whether *CIN1* gene disruption had any effects on the process of sexual reproduction. As depicted, the *cin1* mutant was unable to produce conjugation tubes (Figure 5A). When the *cin1* mutant was crossed to the wild type MAT**a** strain, no mating specific dikaryotic filaments, seen as macroscopic aerial filaments in cross of control strains, were present (Figure 5B). Moreover, the *cin1* mutant failed to initiate hyphal fusion and/or form mating-specific dikaryotic filaments, as demonstrated by a cell fusion assay, which did not yield any colonies in medium supplemented with nourseothricin and neomycin, the markers for MATα and MAT**a** strains, respectively (Figure 5C). The defect in mating could indicate that the *cin1* mutant failed to secrete or sense pheromones because of a defect in the intracellular transport of pheromones (secretion) or pheromone receptors (internalization and recycling), or that the *cin1* mutant was unable to undergo morphogenic transition to form conjugation tubes or dikaryotic filaments.

The cin1 mutant failed to display common virulence traits

Given that the *cin1* mutant exhibited defects in normal morphology as well as in growth and endocytosis, which would inevitably impact its ability to cause infection in experimental animal models, we assessed the ability of the *cin1* mutant to display traits commonly associated with virulence, such as the formation of a polysaccharide capsule and the production of ureases, phospholipase B, and melanin pigment. Obliteration or alteration of any or all of these factors would likely result in attenuated virulence or render the mutant avirulent in animal virulence models.

In Dulbecco's Modified Eagle's Medium (DMEM), the *cin1* mutant was acapsular and displayed characteristic of abnormal morphology, in contrast to the wild type and complemented strains whose capsules were readily visible (Figure 6A).

On Christensen's agar, which readily assesses the production of urease, and egg yolk agar, which detects phospholipase B activity, the *cin1* mutant displayed little growth at 25° C (Christensen's) or no growth at 30° C (Egg yolk) and consequently no urease or phospholipase B production following three days of incubation, in contrast to the wild type strain (Figure 6B). The reconstituted mutant (*cin1 CIN1*) restored growth to the extent of the wild type strain, indicating that the allele is functional and the phenotypic changes were specific to *cin1*.

The *cin1* mutant failed to produce melanin pigment. It demonstrated poor growth in diphenolic compound rich Nigerseed and Asparagine agar media resulting in opaque white colonies upon incubation for three days at 30° C (Figure 6B, Asparagine medium shown). The wild type strain exhibited normally dark pigment, and complementation of the *cin1* mutant with the wild-type *CIN1* allele partially restored melanin production (Figure 6B). Partial restoration in the phenotype by complementation occurs quite frequently in the fungus and is generally attributed to gene dosage or integration positional effect, or the deleterious consequence of multiple transformations (Alspaugh *et al.*, Wang *et al.*, 2002). To confirm that melanin defect is due to secretion rather than lack of cell growth, we assayed the activity of laccase, which is required for melanin formation, using 2,2′-azino-bis(3-ethylbenzthiazoline-6-sulphonic acid, ABTS) as the substrate and cells of equal optical density. Indeed, the laccase activity for the wild-type, *cin1,* and *cin1 CIN1* stains were 30, 2, and 10 units, respectively. This result is consistent with that of the melanin induction assay.

Moreover, we compared the location of a fluorescently labeled laccase protein, Lac1-DsRed, between the *cin1* mutant and wild type strains. Lac1 is predominantly associated with the cell wall under normal conditions, as shown by the presence of fluorescence surrounding cell peripheries of the wild type cell (Figure 7). Incubation in minimal Asparagine medium resulted in more intense fluorescence at the cell periphery and in cytosol (Figure 7). In contrast, fluorescence was seen in the *cin1* mutant cells as unorganized punctate dots or patches and was not seen near the cell periphery (Figure 7), consistent with the earlier observations that the *cin1* mutant is defective in intracellular transport.

The inability to exhibit full virulence traits as the result of *CIN1* gene disruption predicts that virulence is attenuated in the *cin1* mutant or that the *cin1* mutant is avirulent in murine models of cryptococcosis.

Cin1 interacts with Cdc42 and Wsp1

In humans, the ITSN1 RhoGEF domain functions as a GEF to activate Cdc42, a Rho family GTPase, whereas SH3 domains permit interaction with WASP which functions as an effector of Cdc42 to initiate actin filamentation (Symons et al., 1996, Wang et al., 2005, Hussain et al., 2001, Malacombe et al., 2006). Analogously, we hypothesized that one of the Cin1 functions is to maintain the actin cytoskeleton through interactions between the RhoGEF domain and Cdc42, and between the SH3 domains and Wsp1, a cryptococcal homolog of mammalian WASP. To test this hypothesis, we performed a yeast two-hybrid assay to first test the protein-protein interaction. In addition, we created two mutant alleles of Cin1, lacking either RhoGEF or SH3 and RhoGEF domains, and also generated *cdc42* and *wsp1* mutant strains.

Indeed, our results indicated that the RhoGEF domain interacted with Cdc42 and SH3 with Wsp1 through the proline rich domain (Wsp1-PR) (Figure 8A). Surprisingly, none of the

domain-specific mutants exhibited any phenotypes distinct from that of the wild type strain (Figures 3, 6 and 7), in contrast to *cdc42*, *wsp1*, or *cin1* mutants. A certain percentage of *cdc42* and *wsp1* mutants displayed cell separation defects resulting in joint mother and daughter cells, with the percentage and defect less in *cdc42* than in *wsp1* mutants (Figure 8B, phalloidin stain for actin cytoskeleton was shown). This finding suggested that Cdc42 and Wsp1 share a role with Cin1 in control of normal cytokinesis, however, since none of the defects exhibited by *cdc42* and *wsp1* were as severe as that of the *cin1* mutant, the roles of Cdc42 and Wsp1 are likely to be distinct from that of Cin1.

Finally, as a previous study indicated that Ras1 and Cdc24, a putative GEF for Cdc42, function in a pathway mediating thermal tolerance of *C. neoformans* (Nichols *et al*., 2007), we sought to test whether the Cin1 RhoGEF domain has an in vivo activity by compensating for the loss of Cdc24 in thermal resistance, as the *cdc24* mutant cannot grow at 37° C. Under the control of a constitutively activated glyceraldehyde 3-phosphate dehydrogenase (Gpd1) promoter, the expression of the RhoGEF domain nearly restored the growth of the *cdc24* mutants at 37° C (Figure 8C). Collectively, these observations indicate that, while the RhoGEF and SH3 domains may allow Cin1 to interact with proteins contributing to the maintenance of the actin cytoskeleton and signaling, they themselves are dispensable for the pleiotropic function of Cin1, which could be attributed to functional redundancy of proteins containing RhoGEF and SH3 domains.

Discussion

The ability of *C. neoformans* to infect human host causing meningoencephalitis largely depends on its elaboration of virulence factors, which is thought to depend on the endocytic cycle of endocytosis and exocytosis. Previous studies have presented evidence indicating that the membrane vesicles containing GXM, glucosylceramides, ureases, and laccases were all present in this fungus (see review by (Nosanchuk et al., 2008)). In addition, point mutation of the *SAV1* gene encoding Sav1/Sec4 GTPase, a conserved “master” regulator of exocytic transport and silencing of the *SEC6* gene encoding Sec6, a conserved component of the exocytotic vesicle, resulted in either accumulated or disappearance of exosomal vesicles carrying GXM (Yoneda & Doering, 2006, Panepinto et al., 2009). These studies indicated the highly conserved nature of the intracellular transport of membrane particles and provided a glimpse as to the importance of membrane trafficking in growth and virulence of the fungus. Our identification of the multimodular and multifunctional Cin1 allows further studies of membrane trafficking possible in this fungus.

Cin1 exhibits higher domain conservation to human ITSN1 protein than *S. cerevisiae* endocytic protein Pan1, suggesting that Cin1 is likely to have a function similar to ITSN1 in vesicle trafficking, actin dynamics, and signaling. Indeed, disruption of *CIN1* gene resulted in multiple defects in morphology, chitin distribution, growth, endocytosis, mating, and virulence. Importantly, the defects predict that the *cin1* mutant would have an attenuated virulence or be avirulent in animal models. Thus, the multimodular structure capable of linking endocytosis, actin cytoskeleton, and signal transduction may endow Cin1 with a central role in vesicle trafficking and signaling, which is distinct from Sav1/Sec4 or Sec6. Further characterization of Cin1, including its interactions with Sav1/Sec4 and Sec6, would therefore pose a key to understanding how these proteins are coordinated to regulate intracellular trafficking and the transport of virulence “cargos”.

There exist two different isoforms of ITSN1 in humans. The long splicing variant, ITSN1, is expressed only in the brain, and the short splicing variant, ITSN1s, is ubiquitously distributed (Guipponi et al., 1998). Interestingly, a similar short isoform, Cin1s, resulting from alternative splicing of mRNA, also exists in this fungus. The analogy between the

seemingly very divergent organisms is quite astonishing. This analogy, as well as the functional distinction between Cin1 and Cin1s and whether there also exists differentiated distribution or expression, remains to be understood.

To understand how individual modules within Cin1 are organized and their underlying functions, we have begun to characterize individual domain functions, specifically, the C-terminal RhoGEF and SH3 domains. Cin1 was identified through an interaction with the SH3 domain of Gib2, but the functional consequence of this interaction is not known (Palmer et al., 2006). Studies in humans indicated that ITSN1 SH3 domains inhibit the nucleotide exchange activity through a direct interaction of the RhoGEF domain and the blockage of Cdc42 binding (Hussain et al., 2001, Zamanian & Kelly, 2003). Moreover, it is also known that the binding of WASP to ITSN1 through SH3 enhances the RhoGEF's ability to interact with GDP bound Cdc42 (inactive), and to catalyze its conversion to GTP-bound (active) (Hussain et al., 2001). While the constitutive expression of RhoGEF repressed the deficiency of the *cdc24* mutant in thermal resistance suggesting an in vivo activity, apparent phenotypic changes in the Cin1 alleles lacking the RhoGEF and RhoGEF/SH3 domains were not detectable. This dichotomous observation may suggest that these two domains are likely dispensable for Cin1 function, because of the compensatory roles by additional SH3 and GEF containing proteins. Consistent with this view, both Cin1s and ITSN1s lacked the RhoGEF domain indicating that GEF function is not fundamental to the cellular role of the proteins.

Our studies also identified other proteins involved in the control of cytokinesis and cell separation: namely, Cdc42 and Wsp1; Cdc42 appears to have a lesser role than Wsp1. Incidentally, a recent study has suggested that *C. neoformans* Cdc42 (GenBank accession: DQ991433) be changed to Cdc420 and that a protein previously named Dch2 (GenBank accession: DQ991434) be renamed as Cdc42 instead (Ballou *et al.*, 2009). Functional similarity between Cdc42 (Dch2) and Cdc420 (Cdc42) expands the list of potential partners for Cin1 to interact and the functional consequence of these interactions will remain as a very interesting research subject.

Finally, the function of Cin1 is likely to be distinct from that of *S. cerevisiae* Pan1, a homolog of mammalian Eps15 involved in yeast endocytosis through association with adaptor complex AP-2 (Wendland, 1998}. Pan1 coordinates both the structural and regulatory components of the endocytic pathways through interactions with yeast Arp2/Arp3, End3, Yap180, Rsp5, and Sla2 (Wendland & Emr, 1998, Huang & Cai, 2007, Miliaras et al., 2004). A recent inspection of *C. neoformans* revealed the existence of a Pan1/Eps15 homolog (GenBank accession: XP_567624), as well as the potential coding domains for homologs of *S. cerevisiae* Arp2/Arp3 (GenBank accessions: XP_572870/XP_570501), Rsp5 (GenBank accession: XP_572216), and Sla2 (GenBank accession: XP_570853), suggesting a pathway similar to Pan1 may also operate to regulate membrane trafficking and the actin cytoskeleton in *C. neoformans*. Further functional dissections of XP_567624, along with the characterization of Cin1, is therefore warranted.

From these data, we conclude that Cin1 is a novel molecule involved in morphogenic transition, actin dynamics and distribution, membrane or vesicle trafficking, and production or secretion of virulence factors in *C. neoformans*. Cin1 functions in the endocytic cycle of endocytosis and exocytosis, analogous to its mammalian homolog ITSN1 but distinct from *S. cerevisiae* Pan1. The questions of how Cin1 functions and identification of other components of the Cin1 endocytic machinery remain to be addressed. The importance of Cin1-mediated intracellular transport in the display of virulence factors adds additional layer of importance and urgency to the study of Cin1. Moreover, because of the similarity in domain architecture and function between Cin1 and ITSN1, studies of Cin1 may also be

helpful for the understanding of ITSN1 function and its overexpression in the involvement of diseases such as Alzheimer's disease and Down syndrome in humans.

Experimental procedures

Strains, plasmids, DNA sequences, and media

Cryptococcus neoformans var. *neoformans* (serotype D) strains were mostly used in this study and are listed in Supplemental Table 1. The oligonucleotide primers for PCR amplification and sequence verification were synthesized commercially and are listed in Supplemental Table 2. The plasmid DNA constructs are listed in Supplemental Table 3.

cDNA for laccase Lac1 was synthesized with primers PW1481 and PW1482 and fused to the N-terminus of DsRed (Clontech). Once verified by sequencing, the construct for Lac1-DsRed fusion protein was linked to a neomycin resistance cassette and transformed into *C. neoformans* through biolistic transformation. Lac1 is under the control of a glyceraldehyde-3-phosphate dehydrogenase (Gpd1) promoter from *C. neoformans*. Induction and observation of the Lac1-DsRed fusion protein was the same as those previously described (Waterman *et al.*, 2007, Panepinto *et al.*, 2009).

Common media such as Yeast Extract-Peptone-Dextrose (YPD), minimal YNB media, synthetic medium (SD), and media used for analysis of specialized phenotypes, such as filament agar for conjugation tube formation, 10% V8 (pH 5.0) for mating, Niger seed agar and Asparagine for melanin production, Dulbecco's modified Eagle's medium (DMEM) for capsule formation, Christensen's medium for detecting urease activity, and egg yolk medium for phospholipase B, were prepared following standard protocols or as described previously (Wang *et al.*, 2000, Shen *et al.*, 2008, Cox et al., 2000, Price *et al.*, 1982, Chen *et al.*, 1997).

Identification and quantification of Cin1 isoforms

3′ RACE was carried out using a 3′ RACE kit from Invitrogen (Carlsbad, CA) according to the protocol provided by the kit manufacturer. PW700 and PW1127 were used as the 5′ primers and an Abridged Universal Amplification Primer (AUAP) was used as the 3′ primer. A semi-quantitative RT-PCR was performed to estimate the relative abundance of *CIN1* and the splicing variant *CIN1s* transcripts. Briefly, after first strand cDNA synthesis, PCR cycles of 25, 28, and 30 were performed using primers PW1503 and PW1078 (0.47 kb, partial and specific for *CIN1s*), and PW856 and PW857 (0.52 kb, specific for *CIN1*), as well as PW1501 and PW1502 for control (partial actin gene, 0.42 kb). PCR products were gel-separated and transcripts compared using Quantity One 4.4.1 (Bio-Rad Laboratories, Hercules, CA).

CIN1 gene disruption and reconstruction

Alleles for targeted gene disruption were amplified based on a split-marker deletion method (Fairhead *et al.*, 1996). For *CIN1* deletion, the 5′-fragment linking to the 5′ terminus of the nourseothricin acetyltransferase gene (*NAT*) and the 3′ fragment linking with the 3′ terminus of *NAT* were amplified with primers PW600 and PW616, and with primers PW700 and PW701, respectively. The two partially overlapping fragments were then synthesized by overlap PCR with PW600 and PW639 and with PW638 and PW701 (detailed in Figure 1). For the *cin1* mutant linked to the neomycin phosphotransferase gene (*NEO*), the *NAT* marker was replaced by *NEO* through PCR, while other steps remained the same. For RhoGEF domain deletion, the upstream fragment linking to the 5′ terminus of *NAT* and the downstream fragment linking to the 3′ terminus of NAT were first amplified with primers PW1007 and PW1008 and with primers PW617 and PW603, respectively. The two partially

overlapping mutant alleles were synthesized by PCR with primers PW1007 and PW639, and primers PW638 and PW603. For SH3-RhoGEF deletion, the upstream split-marker was obtained by PCR amplification with primers PW1028 and PW1029, and primers PW1028 and PW639, while the downstream split-marker was the same as that for the deletion of the RhoGEF domain (Supplemental Figure 1).

Two approaches were attempted to reconstitute the *cin1* mutant. The first method was the construction of an approximately 10 kb full-length genomic *CIN1* DNA with both the promoter and the terminator sequences amplified with PW738 and PW743. The fragment was ligated to the plasmid pGS200. For unknown reasons, plasmid DNA containing the full-length functional *CIN1* gene could not be obtained. The second method was to divide the full length *CIN1* gene into several fragments and link them one at time. The promoter was amplified with PW738 and PW1073 and inserted into the plasmid pGS302 resulting pGS308. The neomycin cassette was removed from pGS308 by digestion with BamH1 resulting in pGS426. The gene encoding green fluorescence protein (GFP) was inserted in pGS426 resulting in pGS735. The N-terminus of Cin1 amplified with PW1227 and PW1402 was inserted into the TA vector (pGS670) and linked with the coiled-coil domain, amplified with PW1306 and PW1307, resulting in pGS716. The joined piece was cut with BamH1 and Xba1 and inserted into pGS735 to obtain pGS754. The region after the coiled-coil domain was joined from two pieces amplified by PW1393 and PW1394, and PW1078 and PW1396, respectively. This sequence was digested with Spe1 and Not1 and inserted into pGS754 resulting in pGS905. The RhoGEF and PH domains were amplified with PW1397 and AUAP (Invitrogen), and inserted into pGS905 to obtain pGS981. Finally the neomycin cassette was re-inserted into pGS981 resulting in the final plasmid pGS982 that was used for complementing the *cin1* mutant. A diagram of the full-length *CIN1* for complementation is given in Figure 1.

The split-marker alleles were introduced into JEC21 (MATα) and JEC20 (MAT**a**) by biolistic transformation to obtain *cin1* mutants with either the *NAT* or *NEO* marker gene.

Gene disruption for WSP1, CDC42, and CDC24 homologs

The split-marker gene disruption approach was also employed to disrupt *C. neoformans WSP1*, *CDC42*, and *CDC24* genes encoding putative Wsp1, Cdc42, and Cdc24. For *WSP1* disruption, the upstream split-marker was obtained by PCR with primers PW1159 and PW1160, while the downstream split-marker was amplified with primers PW1161 and PW1162. For *CDC42* disruption, the upstream and downstream split-markers were amplified with primers PW1133 and PW1134, and primers PW1135 and PW1136, respectively. For *CDC24* disruption, the upstream and downstream split-markers were amplified with primers PW1141 and PW1142, and primers PW1143 and PW1144, again respectively. The *wsp1*, *cdc42*, and *cdc24* alleles were linked to the *NEO* marker.

All mutants were examined by diagnostic PCR amplification for genotype verification.

Microscopy

Fresh cells grown overnight at 30° C were washed in PBS twice before being subjected to staining with stains/dyes. To stain the nucleus, cells were first fixed and permeabilized with 3.7% formaldehyde and 0.2% Triton X-100 for 30 minutes at room temperature for one hour, washed three times with PBS, then mixed with 0.2 μg/ml DAPI (4′, 6′ diamino-2-phenylindole), applied on polylysine coated slides, and coverslips mounted with nail polish. The nucleus emits cold blue fluorescence under UV excitation. Distribution of chitin and the cell wall were observed by staining cells with calcofluor white (CFW). Cells were incubated with CFW (100 μg/ml) for 15 min, washed once with PBS to remove unbound dye, and

mounted on microslides. For actin staining, cells were first fixed in 3.7% formaldehyde for 30 min at room temperature and permeabilized in 0.2% Triton-X100 prior to incubation with rhodamine-conjugated phalloidin (diluted to 5 μg/ml, Molecular Probes) for 60 min. Cells were then washed with PBS three times and mounted on microslides.

For vesicle and endosome staining, cells were incubated with *N*-(3-triethylammoniumpropyl)-4-(*p*-diethylaminophenyl-hexatrienyl) pyridinium dibromide (FM4-64, 5 μg/ml) for up to 30 minutes allowing uptake of the vital dye (room temperature). Cells were then mounted and observed for fluorescence. All microslides were examined using either an Olympus BX51 fluorescence microscope, or a Zeiss Axio Imager 2 microscope as indicated.

Mutant phenotype characterization

Assays for cell fusion, conjugation tube formation, and mating, as well as melanin and capsule production, were performed as previously described (Wang et al., 2004, Li et al., 2007, Shen et al., 2008, Xue et al., 2006). For laccase activity, cells were grown overnight in YPD (two days for the *cin1* mutant) and concentrations adjusted based on cell density (OD_{600}). The assay condition was the same as before, except that the final concentration of ABTS was 1 mM and the reaction period was 120 min (Wang et al., 2004). One unit of enzyme activity is therefore defined as 0.01 absorbance units at 120 min (A_{420}). For growth, cells were adjusted to the approximate density of OD_{600}= 0.1, serially diluted, and 5 μl spotted onto YPD and YNB plates. Cells were then incubated at 25, 30, and 37° C for three days and photographed.

Urease and phospholipase B activities were detected by culturing mutant and reference strains on Christensen's and egg yolk media, respectively (Cox et al., 2000, Price et al., 1982, Chen et al., 1997).

Yeast two-hybrid assay

For yeast two-hybrid assay, cDNA of the proline rich region of the cryptococcal Wsp1 protein was synthesized using primers PW1287 and PW1288, and inserted into the yeast BD vector pGBKT7. *CDC42* cDNA was synthesized with primers PW863 and PW864, and inserted into the yeast AD vector pGADT7. cDNA for the *CIN1* SH3 domain was amplified with primers PW796 and PW797, and inserted into pGADT7, whereas cDNA for RhoGEF was amplified with PW856 and PW857, and inserted into pGBKT7. Plasmid DNA was transformed into yeast strain AH109 and interactions were assessed according to the method previously described (Palmer et al., 2006, Li et al., 2007).

Supplementary Material

Refer to Web version on PubMed Central for supplementary material.

Acknowledgments

We thank J. Cutler, D. Fox, and anonymous reviewers for critical and helpful comments, S. Martin and P. Calmes for technical assistance, and A. Alspaugh and C. Nichols for sharing unpublished results regarding *C. neoformans* Cdc42 (Cdc420). Gui Shen also wishes to thank T. Doering for helpful suggestions and comments. This research was supported in part by NIH grants (AI054958 and AI074001) and a fund from the Research Institute for Children, New Orleans.

Abbreviations

Cin1	cryptococcal intersectin 1

DH	Dbl homology
DMEM	Dulbecco's Modified Eagle's Medium
EH	Eps15 homology
GEF	guanine nucleotide exchange factor
ITSN1	Intersectin 1
PH	Pleckstrin homology
SH3	Src (cytoplasmic tyrosine kinase) homology 3
WH2	WASP (Wiskott-Aldrich syndrome protein) homology 2

References

Alspaugh JA, Perfect JR, Heitman J. *Cryptococcus neoformans* mating and virulence are regulated by the G-protein alpha subunit GPA1 and cAMP. Genes Dev. 1997; 11:3206–3217. [PubMed: 9389652]

Ballou ER, Nichols CB, Miglia KJ, Kozubowski L, Alspaugh JA. Two CDC42 paralogues modulate *Cryptococcus neoformans* thermotolerance and morphogenesis under host physiological conditions. Mol Microbiol. 2009; 75:763–780. [PubMed: 20025659]

Buchanan KL, Murphy JW. What makes *Cryptococcus neoformans* a pathogen? Emerg Infect Dis. 1998; 4:71–83. [PubMed: 9452400]

Cerione RA, Zheng Y. The Dbl family of oncogenes. Curr Opin Cell Biol. 1996:8.

Chabu CDC. Dap160/intersectin binds and activates aPKC to regulate cell polarity and cell cycle progression. Development. 2008; 135:2739–2746. [PubMed: 18614576]

Chen LC, Blank ES, Casadevall A. Extracellular proteinase activity of *Cryptococcus neoformans*. Clin Diagn Lab Immunol. 1996; 3:570–574. [PubMed: 8877137]

Chen SC, Muller M, Zhou JZ, Wright LC, Sorrell TC. Phospholipase activity in *Cryptococcus neoformans*: a new virulence factor? J Infect Dis. 1997; 175:414–420. [PubMed: 9203663]

Confalonieri S, Di Fiore PP. The Eps15 homology (EH) domain. FEBS Lett. 2002; 513:24–29. [PubMed: 11911876]

Cox GM, Mukherjee J, Cole GT, Casadevall A, Perfect JR. Urease as a virulence factor in experimental cryptococcosis. Infect Immun. 2000; 68:443–448. [PubMed: 10639402]

De Jesus M, Nicola AM, Rodrigues ML, Janbon G, Casadevall A. Capsular localization of the *Cryptococcus neoformans* polysaccharide component galactoxylomannan. Eukaryot Cell. 2009; 8:96–103. [PubMed: 18952901]

Duncan MC, Cope MJ, Goode BL, Wendland B, Drubin DG. Yeast Eps15-like endocytic protein, Pan1p, activates the Arp2/3 complex. Nat Cell Biol. 2001; 3:687–690. [PubMed: 11433303]

Fairhead C, Llorente B, Denis F, Soler M, Dujon B. New vectors for combinatorial deletions in yeast chromosomes and for gap-repair cloning using 'split-marker' recombination. Yeast. 1996; 12:1439–1457. [PubMed: 8948099]

Gasman S, Chasserot-Golaz S, Malacombe M, Way M, Bader MF. Regulated exocytosis in neuroendocrine cells: a role for subplasmalemmal Cdc42/N-WASP-induced actin filaments. Mol Biol Cell. 2004; 15:520–531. [PubMed: 14617808]

Guipponi M, Scott HS, Chen H, Schebesta A, Rossier C, Antonarakis SE. Two isoforms of a human intersectin (ITSN) protein are produced by brain-specific alternative splicing in a stop codon. Genomics. 1998; 53:369–376. [PubMed: 9799604]

Huang B, Cai M. Pan1p: an actin director of endocytosis in yeast. Int J Biochem Cell Biol. 2007; 39:1760–1764. [PubMed: 17303466]

Hussain NK, Jenna S, Glogauer M, Quinn CC, Wasiak S, Guipponi M, Antonarakis SE, Kay BK, Stossel TP, Lamarche-Vane N, McPherson PS. Endocytic protein intersectin-l regulates actin assembly via Cdc42 and N-WASP. Nat Cell Biol. 2001; 3:927–932. [PubMed: 11584276]

Kelly LE, Phillips AM. Molecular and genetic characterization of the interactions between the *Drosophila* stoned-B protein and DAP-160 (intersectin). Biochem J. 2005; 388:195–204. [PubMed: 15631619]

Kopecka M, Gabriel M, Takeo K, Yamaguchi M, Svoboda A, Ohkusu M, Hata K, Yoshida S. Microtubules and actin cytoskeleton in *Cryptococcus neoformans* compared with ascomycetous budding and fission yeasts. Eur J Cell Biol. 2001; 80:303–311. [PubMed: 11370745]

Kozel TR. Virulence factors of *Cryptococcus neoformans*. Trends Microbiol. 1995; 3:295–299. [PubMed: 8528612]

Lengeler KB, Davidson RC, D'Souza C, Harashima T, Shen WC, Wang P, Pan X, Waugh M, Heitman J. Signal transduction cascades regulating fungal development and virulence. Microbiol Mol Biol Rev. 2000; 64:746–785. [PubMed: 11104818]

Li L, Shen G, Zhang ZG, Wang YL, Thompson JK, Wang P. Canonical heterotrimeric G proteins regulating mating and virulence of *Cryptococcus neoformans*. Mol Biol Cell. 2007; 18:4201–4209. [PubMed: 17699592]

Malacombe M, Ceridono M, Calco V, Chasserot-Golaz S, McPherson PS, Bader MF, Gasman S. Intersectin-1L nucleotide exchange factor regulates secretory granule exocytosis by activating Cdc42. EMBO J. 2006; 25:3494–3503. [PubMed: 16874303]

Martina JA, Bonangelino CJ, Aguilar RC, Bonifacino JS. Stonin 2: an adaptor-like protein that interacts with components of the endocytic machinery. J Cell Biol. 2001; 153:1111–1120. [PubMed: 11381094]

Mayer BJ. SH3 domains: complexity in moderation. J Cell Sci. 2001; 114:1253–1263. [PubMed: 11256992]

Miliaras NB, Park JH, Wendland B. The function of the endocytic scaffold protein Pan1p depends on multiple domains. Traffic. 2004; 5:963–978. [PubMed: 15522098]

Mitchell TG, Perfect JR. Cryptococcosis in the era of AIDS - 100 years after the discovery of *Cryptococcus neoformans*. Clinical Microbiol Rev. 1995; 8:515–548. [PubMed: 8665468]

Mohney RP, Das M, Bivona TG, Hanes R, Adams AG, Philips MR, O'Bryan JP. Intersectin activates Ras but stimulates transcription through an independent pathway involving JNK. J Biol Chem. 2003; 278:47038–47045. [PubMed: 12970366]

Nichols CB, Perfect ZH, Alspaugh JA. A Ras1-Cdc24 signal transduction pathway mediates thermotolerance in the fungal pathogen *Cryptococcus neoformans*. Mol Microbiol. 2007; 63:1118–1130. [PubMed: 17233829]

Nosanchuk JD, Nimrichter L, Casadevall A, Rodrigues ML. A role for vesicular transport of macromolecules across cell walls in fungal pathogenesis. Commun Integr Biol. 2008; 1:37–39. [PubMed: 19169363]

Okamoto M, Schoch S, Südhof TC. EHSH1/intersectin, a protein that contains EH and SH3 domains and binds to dynamin and SNAP-25. A protein connection between exocytosis and endocytosis? J Biol Chem. 1999; 274:18446–18454. [PubMed: 10373452]

Palmer DA, Thompson JK, Li L, Prat A, Wang P. Gib2, a novel Gbeta- like/RACK1 homolog, functions as a Gbeta subunit in cAMP signaling and is essential in *Cryptococcus neoformans*. J Biol Chem. 2006; 281:32596–32605. [PubMed: 16950773]

Panepinto J, Komperda K, Frases S, Park YD, Djordjevic JT, Casadevall A, Williamson PR. Sec6-dependent sorting of fungal extracellular exosomes and laccase of *Cryptococcus neoformans*. Mol Microbiol. 2009; 71:1165–1176. [PubMed: 19210702]

Paunola E, Mattila PK, Lappalainen P. WH2 domain: a small, versatile adapter for actin monomers. FEBS Lett. 2002:513. [PubMed: 12435603]

Price MF I, Wilkinson D, Gentry LO. Plate method for detection of phospholipase activity in *Candida albicans*. Sabouraudia. 1982; 20:7–14. [PubMed: 7038928]

Pucharcós C, Fuentes JJ, Casas C, de la Luna S, Alcántara S, Arbonés ML, Soriano E, Estivill X, Pritchard M. Alu-splice cloning of human Intersectin (ITSN), a putative multivalent binding protein expressed in proliferating and differentiating neurons and overexpressed in Down syndrome. Eur J Hum Genet. 1999; 7:704–712. [PubMed: 10482960]

Ram AFJ, Klis FM. Identification of fngal cell wall mutants using susceptibility assays based on Calcofluor white and Congo red. Nature Protocols. 2006; 1:2253–2256.

Rodrigues ML, Nakayasu ES, Oliveira DL, Nimrichter L, Nosanchuk JD, Almeida IC, Casadevall A. Extracellular vesicles produced by *Cryptococcus neoformans* contain protein components associated with virulence. Eukaryot Cell. 2008; 7:58–67. [PubMed: 18039940]

Rohatgi R, Ma L, Miki H, Lopez M, Kirchhausen T, Takenawa T, Kirschner MW. The interaction between N-WASP and the Arp2/3 complex links Cdc42-dependent signals to actin assembly. Cell. 1999; 97:221–231. [PubMed: 10219243]

Roos J, Kelly RB. Dap160, a neural-specific Eps15 homology and multiple SH3 domain-containing protein that interacts with *Drosophila* dynamin. J Biol Chem. 1998; 273:19108–19119. [PubMed: 9668096]

Sengar AS, Wang W, Bishay J, Cohen S, Egan SE. The EH and SH3 domain Ese proteins regulate endocytosis by linking to dynamin and Eps15. EMBO J. 1999; 18:1159–1171. [PubMed: 10064583]

Shen G, Wang YL, Whittington A, Li L, Wang P. The RGS protein Crg2 regulates pheromone and cyclic AMP signaling in *Cryptococcus neoformans*. Eukaryot Cell. 2008; 7:1540–1548. [PubMed: 18658258]

Snapper SB, Takeshima F, Anton I, Liu CH, Thomas SM, Nguyen D, Dudley D, Fraser H, Purich D, Lopez-Ilasaca M, Klein C, Davidson L, Bronson R, Mulligan RC, Southwick F, Geha R, Goldberg MB, Rosen FS, Hartwig JH, Alt FW. N-WASP deficiency reveals distinct pathways for cell surface projections and microbial actin-based motility. Nat Cell Biol. 2001; 3:897–904. [PubMed: 11584271]

Symons M, Derry JM, Karlak B, Jiang S, Lemahieu V, McCormick F, Francke U, Abo A. Wiskott-Aldrich syndrome protein, a novel effector for the GTPase CDC42Hs, is implicated in actin polymerization. Cell. 1996; 84:723–734. [PubMed: 8625410]

Tong XK, Hussain NK, de Heuvel E, Kurakin A, Abi-Jaoude E, Quinn CC, Olson MF, Marais R, Baranes D, Kay BK, McPherson PS. The endocytic protein intersectin is a major binding partner for the Ras exchange factor mSos1 in rat brain. EMBO J. 2000; 19:1263–1271. [PubMed: 10716926]

Vida TA, Emr SD. A new vital stain for visualizing vacuolar membrane dynamics and endocytosis in yeast. J Cell Biol. 1995; 128:779–792. [PubMed: 7533169]

Wang JB, Wu WJ, Cerione RA. Cdc42 and Ras cooperate to mediate cellular transformation by intersectin-L. J Biol Chem. 2005; 280:22883–22891. [PubMed: 15824104]

Wang P, Cutler JE, King J, Palmer D. Mutation of the regulator of G protein signaling Crg1 increases virulence in *Cryptococcus neoformans*. Eukaryot Cell. 2004; 3:1028–1035. [PubMed: 15302835]

Wang P, Heitman J. Signal transduction cascades regulating mating, filamentation, and virulence in *Cryptococcus neoformans*. Curr Opinion Microbiol. 1999; 2:358–362.

Wang P, Nichols CB, Lengeler KB, Cardenas ME, Cox GM, Perfect JR, Heitman J. Mating-type-specific and non-specific PAK kinases play shared and divergent roles in *Cryptococcus neoformans*. Eukaryot Cell. 2002; 1:257–272. [PubMed: 12455960]

Wang P, Perfect JR, Heitman J. The G-protein beta subunit GPB1 is required for mating and haploid fruiting in *Cryptococcus neoformans*. Mol Cell Biol. 2000; 20:352–362. [PubMed: 10594037]

Waterman SR, Hacham M, Panepinto J, Hu GW, Shin SW, Williamson PR. Cell Wall Targeting of Laccase of *Cryptococcus neoformans* during Infection of Mice. Infection and Immunity. 2007; 75:714–722. [PubMed: 17101662]

Wendland B, Emr SD. Pan1p, yeast eps15, functions as a multivalent adaptor that coordinates protein-protein interactions essential for endocytosis. J Cell Biol. 1998; 141:71–84. [PubMed: 9531549]

Xue C, Bahn YS, Cox GM, Heitman J. G Protein-coupled Receptor Gpr4 Senses Amino Acids and Activates the cAMP-PKA Pathway in *Cryptococcus neoformans*. Mol Biol Cell. 2006; 17:667–679. [PubMed: 16291861]

Yamabhai M, Hoffman NG, Hardison NL, McPherson PS, Castagnoli L, Cesareni G, Kay BK. Intersectin, a novel adaptor protein with two Eps15 homology and five Src homology 3 domains. J Biol Chem. 1998; 273:31401–31407. [PubMed: 9813051]

Yoneda A, Doering TL. A eukaryotic capsular polysaccharide is synthesized intracellularly and secreted via exocytosis. Mol Biol Cell. 2006; 17:5131–5140. [PubMed: 17021252]

Zamanian JL, Kelly RB. Intersectin 1L guanine nucleotide exchange activity is regulated by adjacent src homology 3 domains that are also involved in endocytosis. Mol Biol Cell. 2003; 14:1624–1637. [PubMed: 12686614]

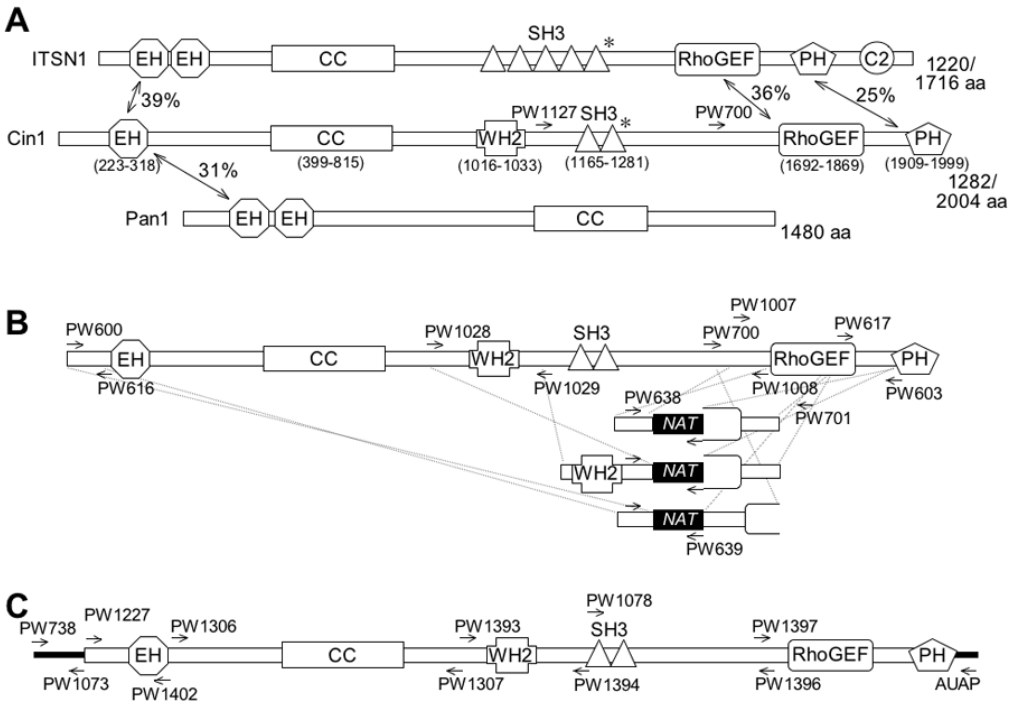

Figure 1.

Schematic representation and domain comparison of *C. neoformans* Cin1, human ITSN1, and *S. cerevisiae* Pan1 proteins (A), schematic representation of the *CIN1* gene full-length, SH3, and RhoGEF domain-specific disruption (B), and the *CIN1* allele for complementation of the *cin1* mutant (C). A) Cin1 contains multiple domains and is more homologous to human intersectin ITSN1 than to *S. cerevisiae* Pan1. Locations of primers PW700 and PW1127 used for 3′ RACE are indicated. Double-ended arrows indicate domain identities in amino acid sequence. Asterisks mark the ends of short protein isoforms due to alternatively spliced mRNAs. Numbers in parentheses indicate aa positions of each domain. GenBank accession numbers for Cin1, Cin1s, ITSN1, ITSN1s, and Pan1 are GU553014, GU586282, AAI16186, AAD299530, and CAB38097, respectively. B) Knock outs of the full-length *CIN1* gene and the alleles without the SH3 and RhoGEF domains. Small single ended arrows mark the location and orientation of primers, which are listed in supplemental Table 2. Dotted lines suggest regions where a DNA double crossover event occurred. C) Construction of a full-length *CIN1* gene for genetic complementation. Arrows mark the location and orientation of primers, also see supplemental Table 2.

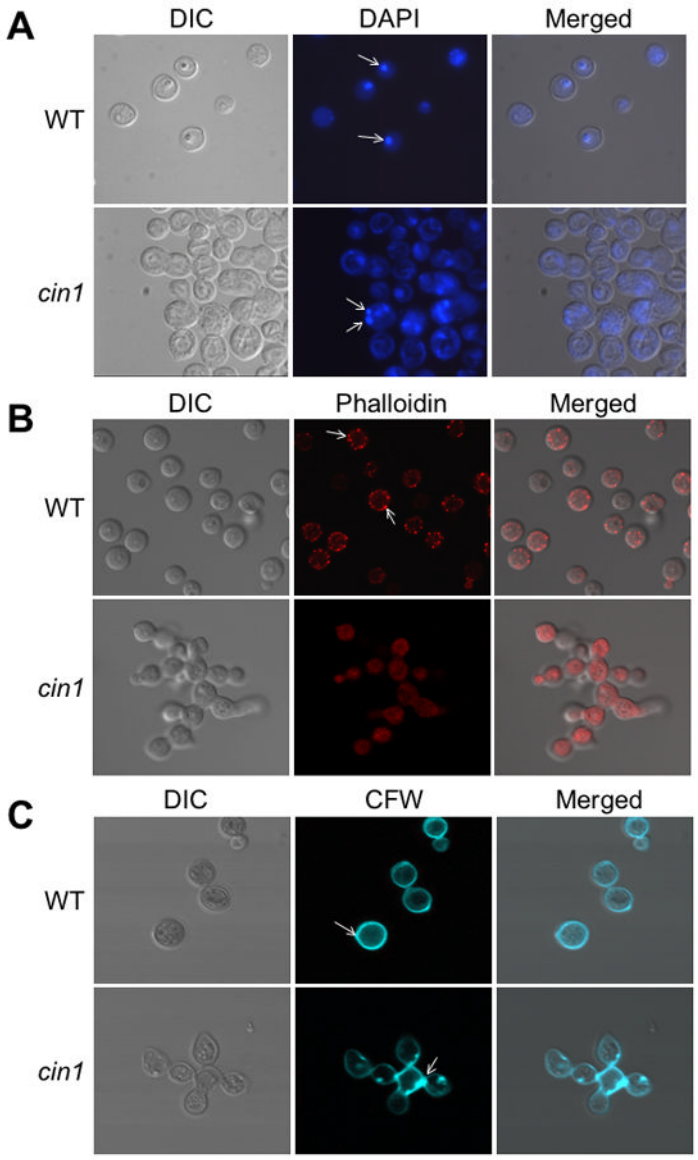

Figure 2.

Cin1 is required for normal morphogenesis of *C. neoformans*. A) The *cin1* mutant and wild type JEC21 strains grown in YPD overnight were stained with DAPI. Arrow bars point to nuclei. B) Rhodamine-conjugated phalloidin staining for the actin cytoskeleton. Arrow bars indicate actin patches. C) Calcofluor white (CFW) staining for chitin and cell walls. Arrow bars point to the bud scar or bud neck. Samples were observed under an Olympus BX51 fluorescence microscope and representative images were captured using a digital camera equipped with the microscope.

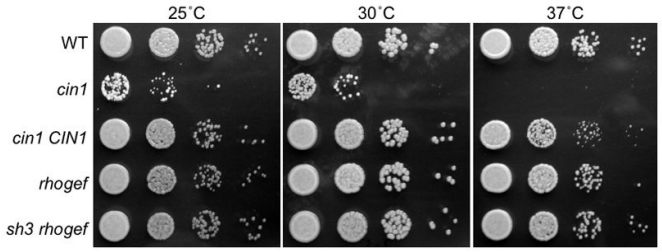

Figure 3.

The *cin1* mutant exhibits a growth defect. The *cin1, cin1 CIN1, CIN1-rhogef, CIN1-sh3-rhogef* and wild type cells grown overnight in YPD were adjusted to an optical density of approximately 0.1 (OD_{600}), serially diluted, and 5 μl of cell suspensions were spotted to fresh YPD. Plates were incubated at 25° C, 30° C, and 37° C respectively for three days and photographed.

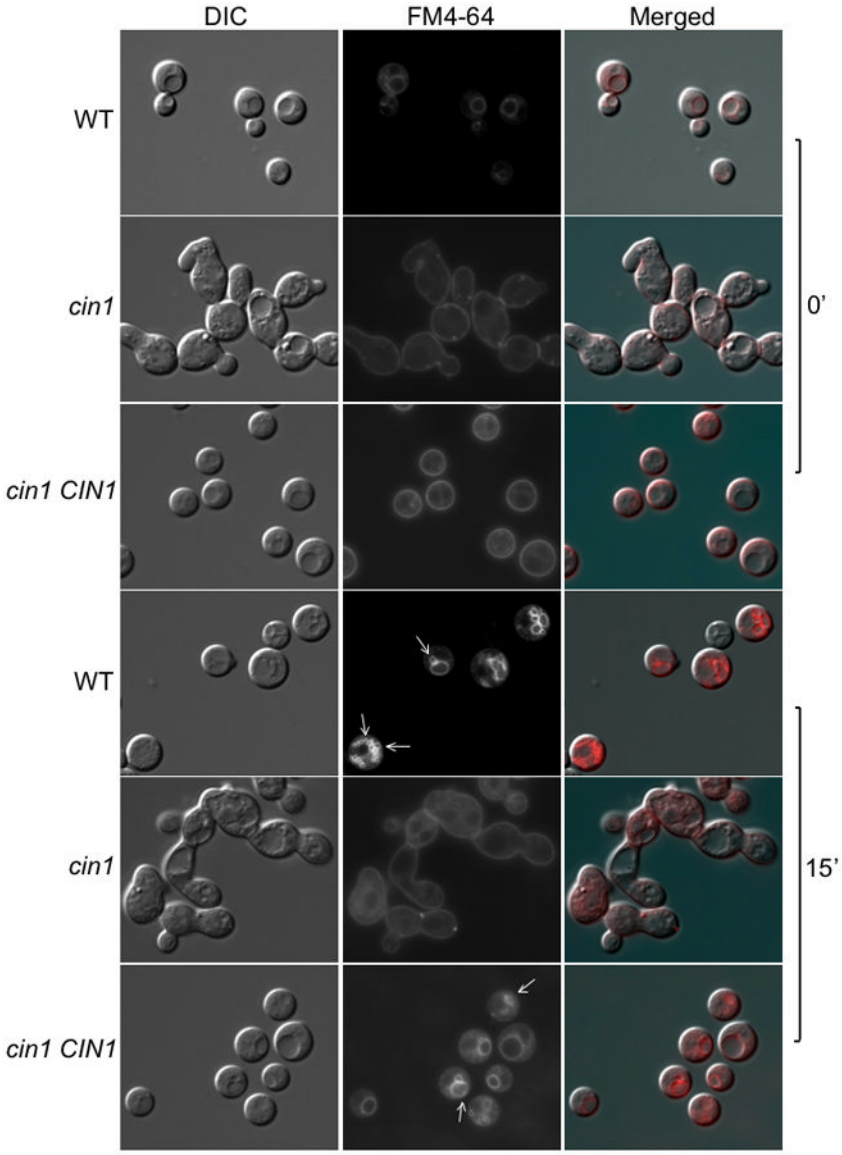

Figure 4.

The *cin1* mutant exhibits a defect in endocytosis. Cells were stained with membrane marker FM4-64 and incubated for a period of time (minutes) as indicated before being examined under the microscope. The *cin1* mutant, wild type (JEC21), and complemented (*cin1 CIN1*) strains grown overnight at 30° C were washed with distilled sterile water and incubated with FM4-64 for up to 15 minutes in order for it to be internalized into the endosomes, which appear as small bright ring-like structures. The changes in the pattern of the *cin1* mutant indicate that the endocytic process failed to occur. Arrow bars point to endosomes. The images were obtained using a Zeiss Axio Imager 2 microscope.

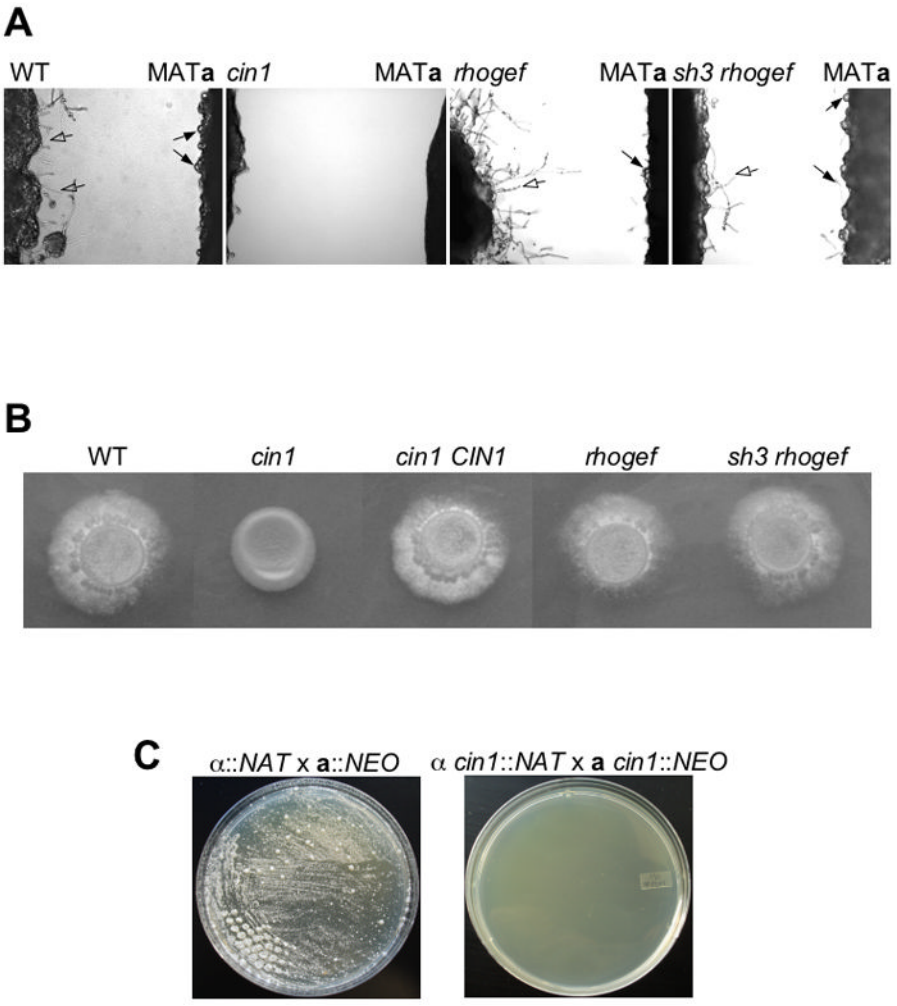

Figure 5.

C. neoformans Cin1 is required for mating. A) The *cin1* mutant is defective in the formation of conjugation tubes (boxed arrows) and the promotion of pheromone responses of the opposite mating type cells, as indicated by solid arrows pointing to swollen cells and/or short conjugation tubes. The *cin1*, *CIN1-rhogef*, *CIN1-sh3-rhogef*, and wild type cells were streaked along side of the MAT**a** strain (JEC20) without touching. After incubation for 48 hours at 25° C, representative sections were photographed. B) The *cin1* mutant is sterile. Aerial views of mixed MATα and MAT**a** cells depict fuzzy projections surrounding colonies, such as that of the wild type strain, but not the *cin1* mutant. These fuzzy projections are mating-specific dikaryotic filaments. C) The *cin1* mutant is defective in cell fusion. Wild type MATα cells (JEC21) were transformed with the *NAT* marker gene for nourseothricin resistance, whereas MAT**a** cells (JEC20) were rendered resistant to G418 by transforming with the *NEO* marker gene. The MATα and MAT**a** cells were mixed for 12 hours, serial diluted, and plated onto medium containing both nourseothricin and neomycin. Following fusion, dikaryotic cells containing both wild type MATα and MAT**a** cells were able to grow, as shown in the left panel.

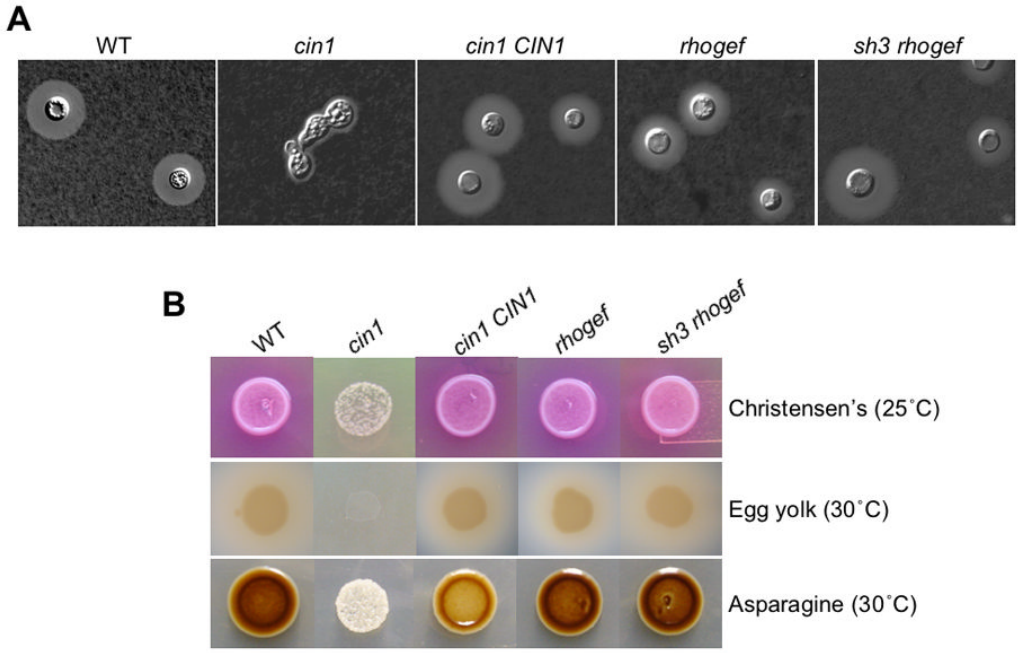

Figure 6.

Disruption of the *CIN1* gene results in defects in virulence traits. A) The *cin1* mutant is also acapsular. The *cin1*, *cin1 CIN1*, *CIN1-rhogef*, *CIN1-sh3-rhogef*, and wild type mutants were grown in liquid DMEM medium for three days. No capsule formation was observed in the *cin1* mutant, which also exhibits morphology defect, in contrast to other strains. Cells were incubated in a shaker (225 rpm) for two days at 30° C. B) At 30° C, the *cin1* mutant grew little on Christensen's medium for the detection of urease production, as indicated by lack of the pink color in medium which surrounds colonies of the wild-type, domain-specific mutant allele, and complemented strains (middle row). At 25° C, the *cin1* mutant failed to grow on egg yolk medium for the production of phospholipase, whereas other strains produced normal levels of phospholipase B, as indicated by colony color and surrounding halos. Colonies were incubated for two days at the indicated temperatures.

The *cin1* mutant also failed to produce melanin pigment on Asparagine agar, indicating a defect in melanin production. In comparison, wild type JEC21 strain and two domain specific mutant alleles, *CIN1-rhogef* and *CIN1-sh3-rhogef*, exhibited normal melanin pigment. Melanin formation is partially restored in the *cin1* mutant strain reconstituted with full-length *CIN1* gene (*cin1 CIN1*). Colonies were incubated for two days at the indicated temperature.

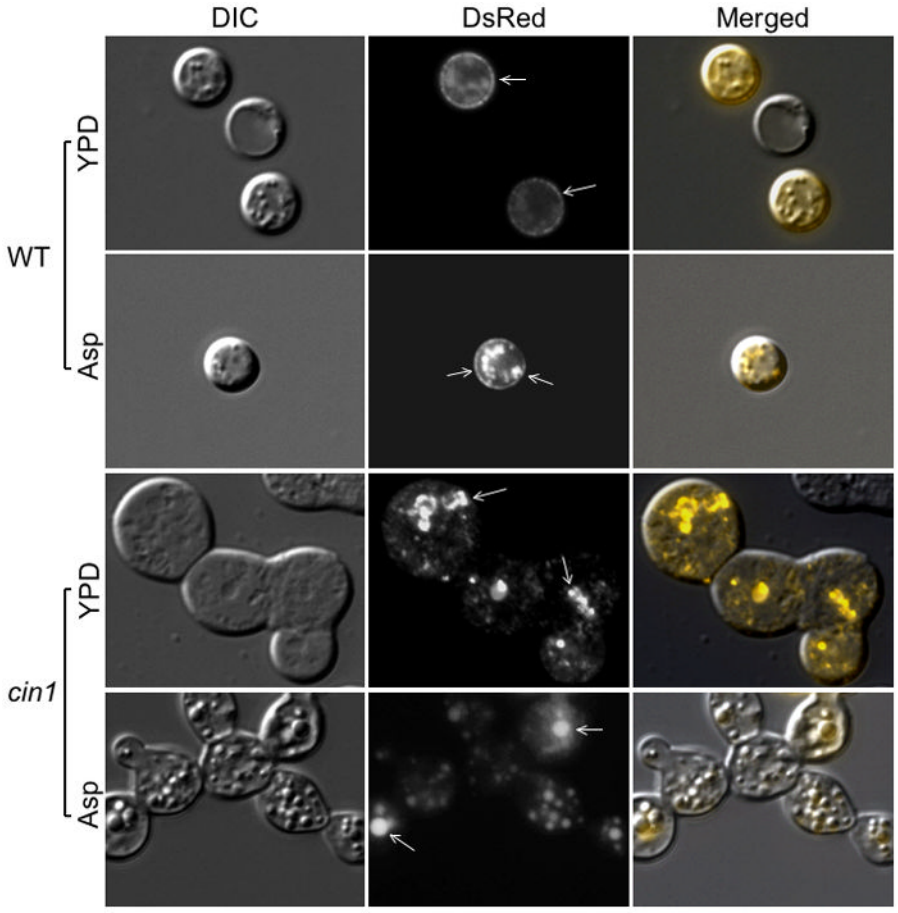

Figure 7.
Cin1 is required for intracellular transport of Lac1. Cells expressing the Lac1-RsDed construct were grown in YPD overnight, washed with distilled sterile water, and either mounted to microslides or re-suspended in minimal Asparagine induction media for additional 24 hours at 30 C. Cells were examined by epifluorescence microscopy using a Zeiss Axio Imager 2 microscope. Arrows point to areas where the Lac1-DsRed protein is located.

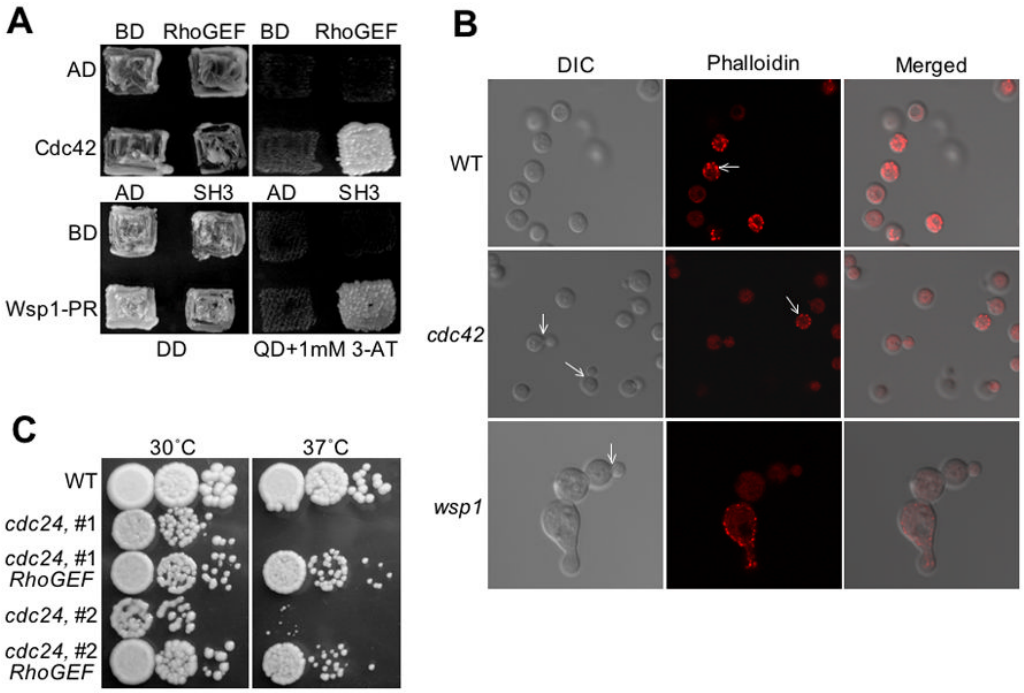

Figure 8.

Cin1 interacts with cryptococcal Cdc42 and Wsp1, a homolog of mammalian WASP, through the RhoGEF and SH3 domains, respectively. A) The RhoGEF domain binds to Cdc42, whereas the proline-rich domain of Wsp1 (Wsp1-PR) binds to SH3, in a yeast two-hybrid assay. cDNA for Cdc42 was cloned into pGADT7 and the RhoGEF was ligated into pGBKT7. Similarly, the Wsp1-PR region was cloned into pGBKT7, while cDNA for SH3 (x2) was cloned into pGADT7. Yeast transformants were patched onto double dropout medium (DD) and then colony-replicated onto quadruple dropout medium (QD) plus 3-AT. B) *cdc42* and *wsp1* mutants showed defects in cytokinesis, and *cdc42*, but not *wsp1*, exhibited near normal distribution of actin patches following staining by rhodamine-conjugated phalloidin. Cell stains were observed under an Olympus microscope and images captured with a digital camera equipped with the microscope. Arrows point to joined mother and daughter cells (DIC) and actin patches (Phalloidin). C) Constitutive expression of the RhoGEF domain from Cin1 restores thermal tolerance to the mutant strain of *cdc24*. Two independent *cdc24* and *cdc24* RhoGEF strains were included in the growth assay.